

The VISTA Infrared Camera

G.B. Dalton^{*a,f}, M. Caldwell^a, A.K. Ward^a, M.S. Whalley^a, G. Woodhouse^a, R.L. Edeson^a, P. Clark^b, S.M. Beard^c, A.M. Gallie^c, S.P. Todd^c, J.M.D. Strachan^c, N.N. Bezawada^c, W.J. Sutherland^d, and J.P. Emerson^e

^aSpace Science and Technology Dept., CCLRC Rutherford Appleton Laboratory, Chilton, Didcot, OX11 0QX, UK;

^bDept. of Physics, University of Durham, South Road, Durham, DH1 3LE, UK ; ^cUKATC, Blackford Hill, Edinburgh, EH9 3HJ, UK ; ^dInstitute of Astronomy, Madingley Road, Cambridge, CB3 0HA; ^eAstronomy Unit, Queen Mary University of London, Mile End Road, London, E1 4NS; ^fDepartment of Physics, University of Oxford, Keble Road, Oxford, OX1 3RH, UK.

ABSTRACT

We describe the integration and test phase of the construction of the VISTA Infrared Camera, a 64 Megapixel, 1.65 degree field of view 0.9-2.4 micron camera which will soon be operating at the cassegrain focus of the 4m VISTA telescope. The camera incorporates sixteen IR detectors and six CCD detectors which are used to provide autoguiding and wavefront sensing information to the VISTA telescope control system.

Keywords: Infrared Astronomy; Survey Astronomy; Infrared Detectors; Large Lenses; Active Optics

1. INTRODUCTION

The Visible and Infrared Survey Telescope for Astronomy (VISTA)^{1,2,3} is a 4 metre wide-field telescope that is purpose-designed for deep astronomical imaging surveys in the near-infrared and visible. The telescope design caters for interchangeable instruments mounted at the f/3.25 Cassegrain focus with the assumption that each instrument will provide its own purpose-specific wide-field correcting optics. VISTA will be located at ESO's Paranal Observatory, 1.5km from the VLT.

The IR Camera will operate on the VISTA telescope, utilizing a 1.65 degree field of view with a complement of 16 2048×2048 Raytheon VIRGO HgCdTe arrays⁴ giving 0.34 arcseconds per pixel in the science focal plane with good imaging performance between 0.9µm and 2.5µm. The camera is roughly 3m in length, has a total mass of 2,900kg, and will be the largest infrared camera ever built, both in terms of field of view and number of detector pixels.

The wide-field design of the telescope requires active control of the position and tilt of the secondary mirror, and the camera also includes a pair of onboard curvature sensors as well as frame-transfer CCDs for autoguiding. In the first instance VISTA will be operated as a single instrument telescope, and so the IR Camera is designed for continuous operation between scheduled yearly downtimes for essential maintenance.

The camera is now essentially complete in the assembly, integration and verification (AIV) facility at the Rutherford Appleton Laboratory undergoing final testing and awaiting shipping to Chile for integration and commissioning which is now expected to commence in November of 2006. This paper will cover the evolution of the design⁵ into the final build, some lessons that can be learned from the build process of such a large cryogenic instrument, and those performances of the instrument which have been measured in the laboratory.

2. INSTRUMENT OVERVIEW

When in position on the telescope (Figure 1), the IR Camera provides image correction for the telescope's f/3.25 focused beam, over its wide field of view (FOV) of 1.65 degrees diameter. This image correction includes:

* G.B.Dalton@rl.ac.uk

- Removal of field curvature to allow a large planar array of detectors to be used (350mm diameter), while controlling the off-axis aberrations and chromatic effects using system of three lenses.
- Autoguiding and wave-front sensing of the beam⁶ for the purpose of active optics control in the telescope⁷ to correct flexure and other opto-mechanical effects arising from both the telescope and camera parts of the system.

The camera produces no intermediate imaging (Figure 1), and has low optical power, so that the position of the final focal plane with the camera present is close to that of the telescope when the camera is absent.

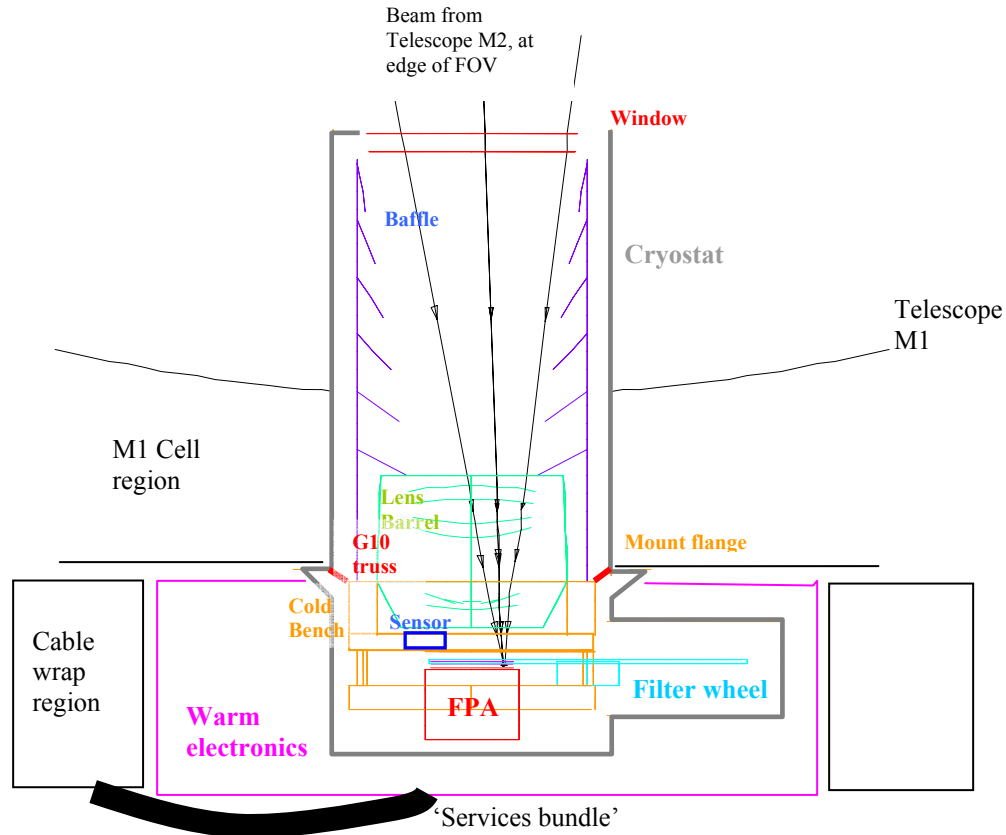


Figure 1: General view of the VISTA infrared camera layout

The specification on the net imaging performance of the system is for point spread function of width compatible with the detectors pixel size (0.34'') over this wide FOV and over wavelength range 1.0 to 2.35 μ m. The spectral channels in this range (Y to Ks) are defined by filters in a wheel positioned close to the focal plane. This has slots for up to seven science channels and the filter sets for these can be changed during off-telescope maintenance. The eighth slot in the wheel contains a blanking plate for dark calibrations as the focal plane has no shutter assembly.

3. MECHANICAL STRUCTURE

3.1 Mechanics and Metrology

The cryostat was completed and vacuum tested (Fig 1a) at NTE Ltd. (Poole, UK) in December of 2004. The aluminium cryostat is built in four main sections, and includes over 10m of O-ring seals. After extensive cleaning and outgassing at elevated temperature, the cryostat vessel was found to reach a stable vacuum at the level of 10⁻⁶mb at room temperature. The cryostat heat-shields are made from 2mm polished stainless steel plate and these are fitted to the inner walls of the

vessel sections with GFRP stand-offs. The centre-section heat shield was found to be a poor fit, and measurement of the centre-section revealed that the inner diameter was 10mm smaller than the design. Extensive discussions with NTE led to the conclusion that this error was the result of shrinkage of the section during manufacture due to the large number of welds required to incorporate vacuum ports (see Fig 2c) and stiffening ribs into this section. The centre section heat-shield was modified by cutting it into three overlapping sections.

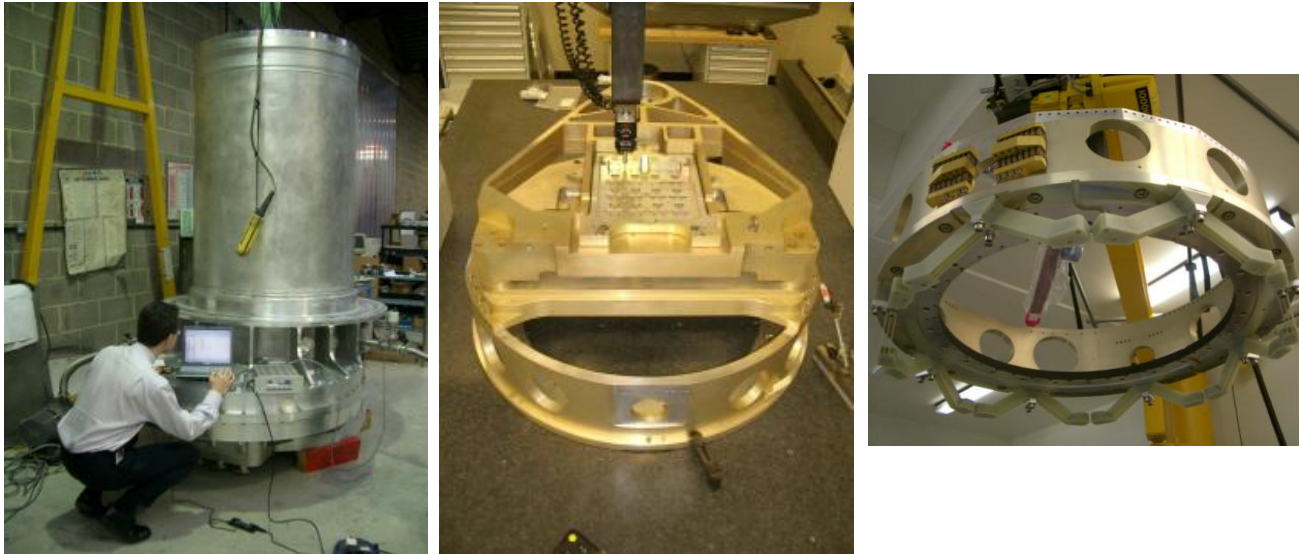


Figure 2: (a) The cryostat vessel at NTE undergoing vacuum testing. (b) The four major internal sections of the cryostat cold assembly on the CMM machine at RAL. (c) The optical bench section being lowered into the cryostat (upside down!), showing the GFRP trusses that support all the cold mass from the cryostat centre-section. The gold parts at centre left are part of the cold strap harness that links to the cooler units.

A key issue throughout the design of the IR Camera was the tight tolerance required for the alignment of the whole system⁶, both within the cold assembly ($50\mu\text{m}$ between the aO sensors and the focal plane), and between the cold assembly and the Cassegrain rotator flange of the telescope ($50\mu\text{m}$ between the focal plane and the telescope mount). Given a cold assembly mass of around 900kg, this has required careful consideration. Detailed metrology of the assembly of the four main cold sections (Fig 2b) showed that it was possible to replace the Focal Plane support plate to within $4\mu\text{m}$ of its nominal position.

3.2 Vacuum and Cryogenics

The IR Camera is designed with the intent that it will remain in operation at cryogenic temperatures for a full year on the telescope, with a minimum annual downtime scheduled for preventative maintenance and any filter changes. Initial pump-down of the system is achieved using a roughing pump housed in a trolley available either in the instrument preparation lab or the telescope observing floor. Full vacuum is achieved with a pair of He closed cycle cryopumps that are permanently mounted on the camera centre-section. Once the instrument is cold these are valved-off by means of electrically operated gate-valves and purged so that they can be used to recover from any long-term degradation of the vacuum during the operational cycle. The cryopumps are operated from the same services trolley as the roughing pump.

During operation the camera is maintained at temperature by means of 3 Leybold Coolpower 5/100T cold heads mounted to the centre-section. The second stages of these three units are linked directly to the focal plane assembly. These are capable of maintaining operational temperatures for the camera, and will provide satisfactory operation in the event that a single unit should fail. Actual cooldown of the system is achieved by flowing liquid nitrogen into a tube that is mounted to the inside of the optical bench section. This is controlled by an automated system that connects to a pair of 120 litre dewars and cycles liquid nitrogen into the cold tank in short bursts which are allowed to boil off to 4 bar

before the gas is released to an exhaust vent outside the VISTA enclosure. This system reduces the total cooldown time for the camera from around 10 days using just the cold heads to 3 days using liquid nitrogen (8 dewars), with the final rate being limited by the desire not to impose excessive thermal gradients on the lens barrel. The internal tank and filling system are shown in Fig 3.

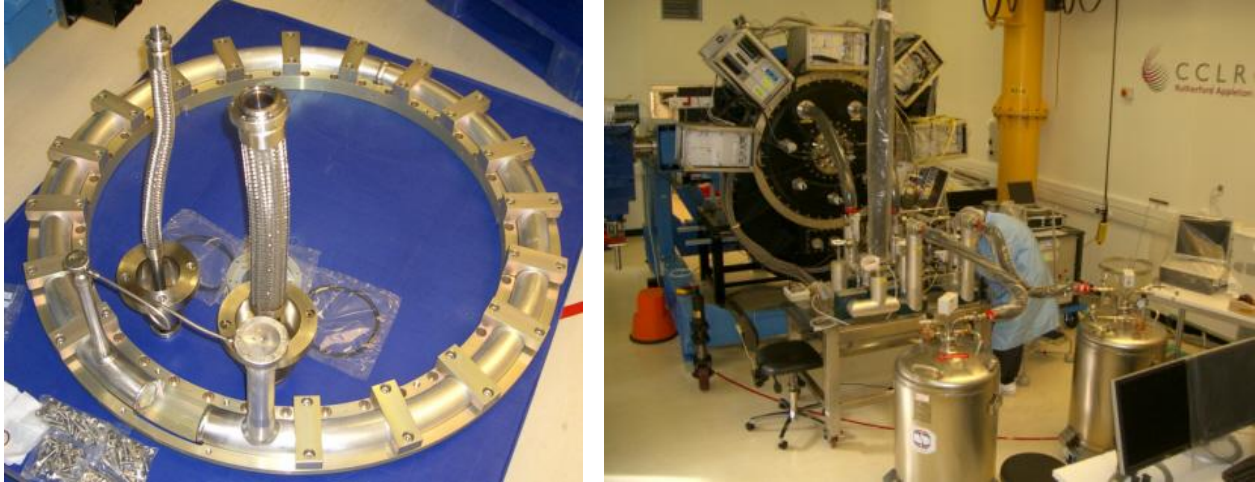


Figure 3: a) The liquid nitrogen tank which bolts to the underside of the optical bench. b) The automated liquid nitrogen filling system which is used to pre-cool the camera.

4. OPTICS

4.1 Lens Barrel

The three infrasil lenses that make up the VISTA IR field corrector were manufactured and coated by SAGEM and delivered to UKATC for assembly into the lens barrel. Each lens is mounted between a PTFE ring, and an aluminium surface, and supported radially by twelve PTFE pistons. In practice, this will lead to three points of contact between the lens and the Al surface, which will in turn lead to thermal gradients within the lens. Detailed modelling of this effect shows a trefoil shaped temperature variation in the lens with a peak-valley range at operating temperature of 8.2K in the lens closest to the window, of which 3.1K is within the region of the lens utilised by the science beam. Given the dn/dt of fused silica of $6 \times 10^{-6} \text{ K}^{-1}$ at operating temperature, this gives a focus offset and a residual wavefront error which degrades the image quality by $0.05''$ in the Ks band and $0.11''$ in the Y band, which dominates the contribution to the overall image quality from the lens barrel internal stability. In order to reduce this contribution the design was modified to include a copper strap across the contact between each PTFE piston and the lens edge. This changes the symmetry of the temperature gradients in the lens from three-fold to twelve-fold and reduces the overall peak-valley temperature inhomogeneity in the lens to 2.8K, of which only 1.3K is within the region of the lens utilised by the science beam. The corresponding image quality terms are reduced to $0.022''$ in the Ks band and $0.046''$ in the Y band. The magnitude of this effect in the Ks band is now reduced to the same level as the term arising from the mechanical deformation of the lens due to the 3-point contact on the Al mounting surface.

4.2 Filter Wheel

The 1.4m diameter Al filter wheel has one dark panel, 7 slots for science filters, and 8 small slots between the science filters which can be used for engineering purposes and wavefront sensing. In the default configuration there will be five broadband science filters covering Z_{IR}, Y, J, H, Ks , with the two remaining slots initially left dark, but available for additional filters to be added if desired. Each science filter is built up from 16 individual 54mm square glass filters (one for each detector) up to 17mm thick, held in a custom tray by GFRP springs and retaining clamps. The wheel is driven by a stepper motor that has been prepared for cryogenic use and provides 210,000 steps per revolution. Filters can be

loaded into the wheel through an access hatch in the upper surface of the filter wheel bulge in the cryostat. The wheel positioning is repeatable to within a single step over 10 revolutions. The wheel positioning software includes knowledge of the approximate transparency of each filter, and will attempt to avoid crossing ‘bright’ filters when moving between ‘faint’ (e.g. narrow band) filters, provided that the wheel population has been arranged effectively. The time required for a full revolution of the wheel is around 30s.

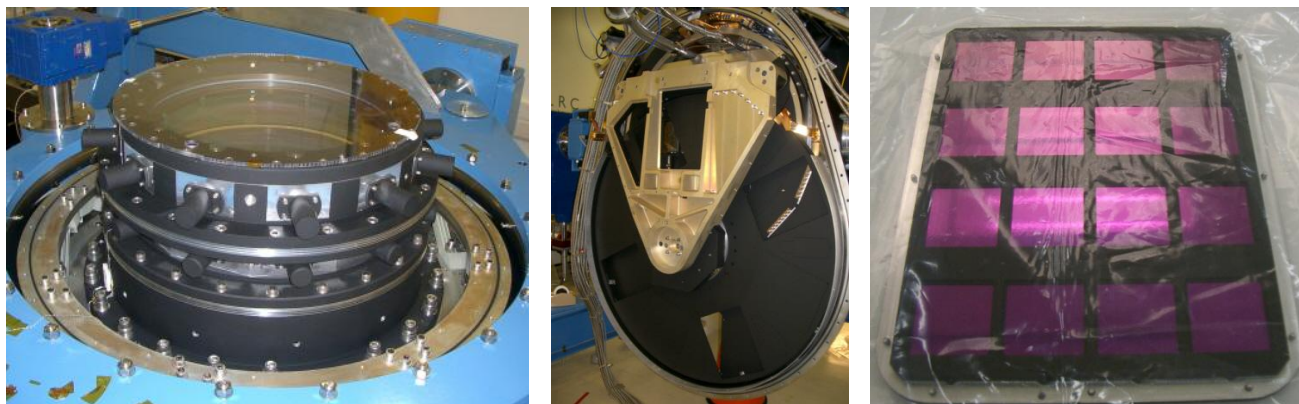


Figure 4: a) The lens assembly mounted to the top of the optical bench. b) the filter wheel installed in the camera (The triangular sections in the focal plane support plate are access panels to allow removal of the wavefront sensor units for maintenance. c) The J science filter ready for installation.

4.3 Baffle system

Unlike most astronomical cameras working into the $2.2\mu\text{m}$ wavelength regime, VISTA has no re-imaging optics or cold pupil stop. Instead, the camera uses a set of seven nested cold baffles to block out of beam radiation. In addition, the baffles serve to reject the unwanted heat load from the window by means of a specialised coating⁵ which is highly absorbing at wavelengths shortward of $3\mu\text{m}$ and highly reflective longward of $3\mu\text{m}$. For this coating to be effective, the baffles themselves were machined to a set of elliptical surfaces. The rear surface of each baffle is painted with the same absorbing black paint (Z306) as the rest of the cryostat interior. The baffles are built up onto the upper surface of the optical bench to form a $\sim 1.8\text{m}$ long tubular assembly which is then enclosed by the outer cryostat tube and heat shield (Figure 5b). The size of this assembly and the proximity of the first surface to the cryostat window meant that great care had to be taken with warm and cold dimensions during the design to ensure both correct positioning of each baffle, and that the cryostat can actually be assembled at room temperature.

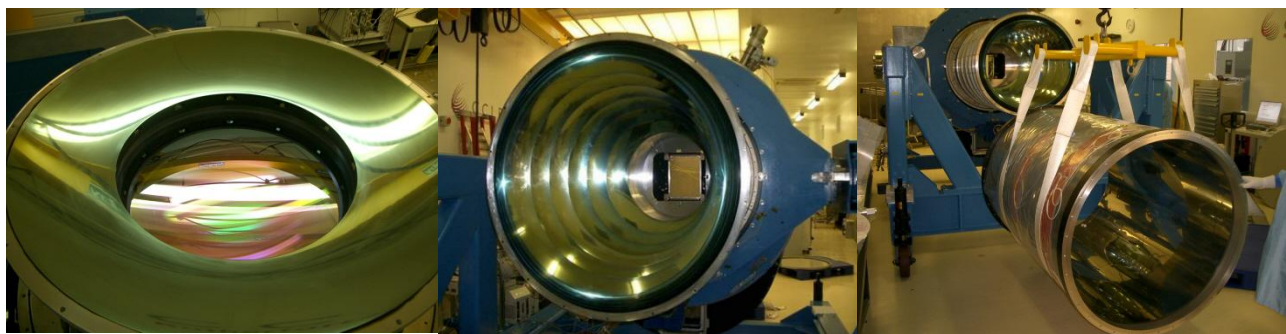


Figure 5: a) The first baffle after coating at Reynard Corp. b) The full baffle assembly attached to the optical bench. c) Lifting the cryostat tube into place.

4.4 Window

The cryostat window represents one of the most challenging aspects of the VISTA design. The window is 950mm diameter and 80mm thick, made from Heraeus Infrasil IR grade fused silica. This is a larger diameter and volume of

material than the largest ingot that Heraeus could manufacture, and so a double length ingot was fabricated by Heraeus by annealing two 300x550mm ingots together. This was then shipped to Corning to be flowed out into a blank of around 1m diameter before finally shipping to Sagem for grinding and polishing to produce the final window. From start to finish this process took a full two years before the finished window was delivered to RAL for integration into the camera. During the early stages of the camera integration, we therefore procured a 600mm BK7 window for testing of the window cell mounting procedures, and to allow optical measurements to be made of the camera internals.



Figure 6: a) The merged infrasil blank (605x550mm) undergoing homogeneity testing at Heraeus. b) The flowed out 1m blank at Corning prior to shipping to Sagem for polishing. c) The final 950x80mm cryostat window mounted in its cell ready for wiring up of the heater circuit.

5. FOCAL PLANE

The VISTA IR focal plane array (FPA) is populated with 16 Raytheon VIRGO 2048x2048 HgCdTe arrays in a sparse mosaic configuration (Figure 7a). These are mounted on a Molybdenum plate which is supported from the FPA frame (upper component in Figure 2b) on three Titanium flexure blades. The requirement on the flatness of the array is that all pixels should be located between two planes separated by $25\mu\text{m}$ along the optical axis of the camera. The detectors each read out through 16 outputs. All detectors are read out simultaneously by an enhanced version of ESO's IRACE IR controller⁹, with a total of 256 simultaneous readout channels. The readout time for the full array is 1s, and this is the minimum exposure time for the camera. The cold part of the readout electronics is located in four PCBs that run back from the rear of the FPA frame to a single flange on the lower ring of the cryostat. The full focal plane assembly from the detectors to this flange can be removed from the rear of the camera as a single unit with a mass of close to 70kg (Figure 7b).

For the 16 science detectors, the mean quantum efficiencies have been measured as (J,H,K)=(90,96,92)%, the mean dark current is $1.2\text{ e}^-\text{pix}^{-1}\text{s}^{-1}$ and the mean readout noise is 20.9 e^- . Quantum efficiencies were measured in the Z and Y bands for a single detector, giving 70% and 80%, respectively, which are expected to be representative of the full set of 16. Well-depths for the arrays (defined as the point at which the non-linearity of the response exceeds 5%) range between 110,000 and 180,000 e^- .

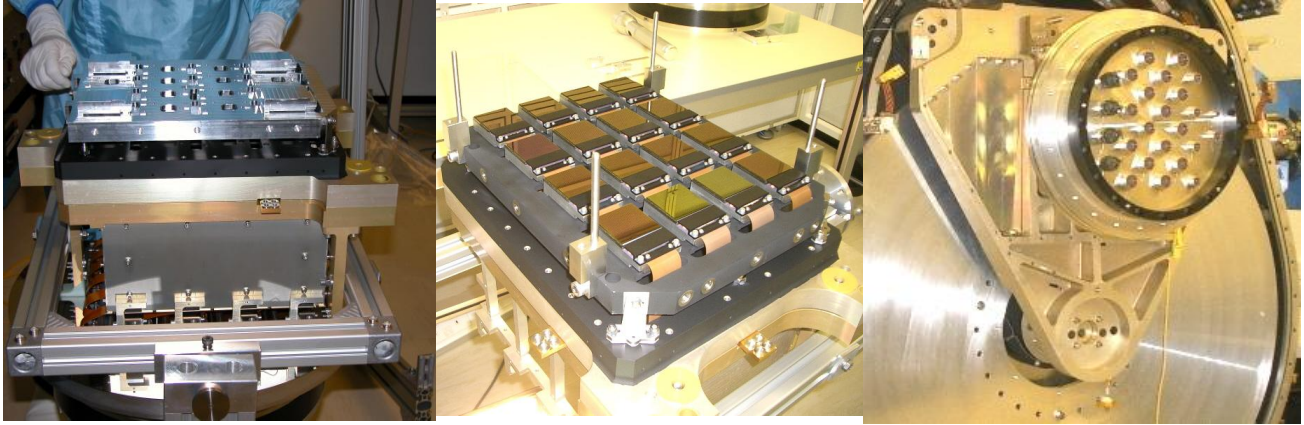


Figure 7: a) Trial build of the FPA 'keg' with Al dummies for the mounting plate and the detectors. b) The fully assembled focal plane located on its titanium blade flexures. c) The 'keg' mounted to the FPA support frame showing the lower vacuum flange.

6. AUTOGUIDER & WAVEFRONT SENSORS

The extremely fast design of the VISTA telescope optics implies stringent stability requirements on the alignment of the telescope mirrors and the instrument. This stability is achieved by means of active correction of the position (3-axis translation, tip and tilt) of the secondary mirror. Given the wide-field specification, the feedback sensors for these corrections are located in two units (referred to as Low Order Curvature Sensors/Autoguiders, or LOCS/AGs) within the camera. The units are located above the filter wheel assembly, and sample the beam at the edge of the corrected field of view. Each unit contains three e2v technologies CCD42-40 2048x2048 CCDs, the first of which has a frame-transfer mask and a 1024x1024 pixel useable area. This is used to provide auto-guiding capability for the telescope at up to 10Hz frame rate for a 100x100 pixel window. The other two devices have 2048x2048 useful pixels, and are mounted at the two outputs of a cuboid beamsplitter arrangement which provides pre- and post-focal images of a suitable star which are used to analyze the curvature of the wavefront⁶.

The system is further complicated by the fact that the LOCS/AG units logically reside within the telescope control system (TCS) rather than the instrument control system (ICS) from a software perspective⁷. The LOCSs are designed to provide information on Focus, Coma and Astigmatism terms to allow correction of the position of the telescope secondary mirror on a timescale of ~1 minute. The use of a pair of LOCSs allows the system to differentiate between astigmatism introduced by mis-alignment of the secondary mirror and astigmatism introduced by incorrect (open-loop) control of the shape of the primary mirror. A higher-order curvature sensor which can determine primary mirror aberrations up to Z_{26} is implemented within the camera by means of a beam splitter located in the filter wheel in the otherwise dead space between two of the science filters.

The LOCS/AG units are designed as self-contained subsystems which are mounted between the final lens and the filter wheel assembly. The units are fed by means of pickoff mirrors, constructed such that the LOCS/AG fields of view are within the unvignetted focal planes, but do not incur vignetting of the science detectors. The units can be removed for maintenance by removing the lower ring of the cryostat, removing one filter[‡], and opening a hatch in the wavefront sensor support frame (wedge-shaped opening in Figure 4b). Each LOCS/AG unit is controlled by two ESO TCCD systems based on SDSU III controllers, such that the AG and CS subsystems remain logically separate.

[‡] In practice, two opposing filters must be removed for this operation as the wheel cannot be driven out-of-balance when the camera is horizon pointing for access to the LOCS/AG units.

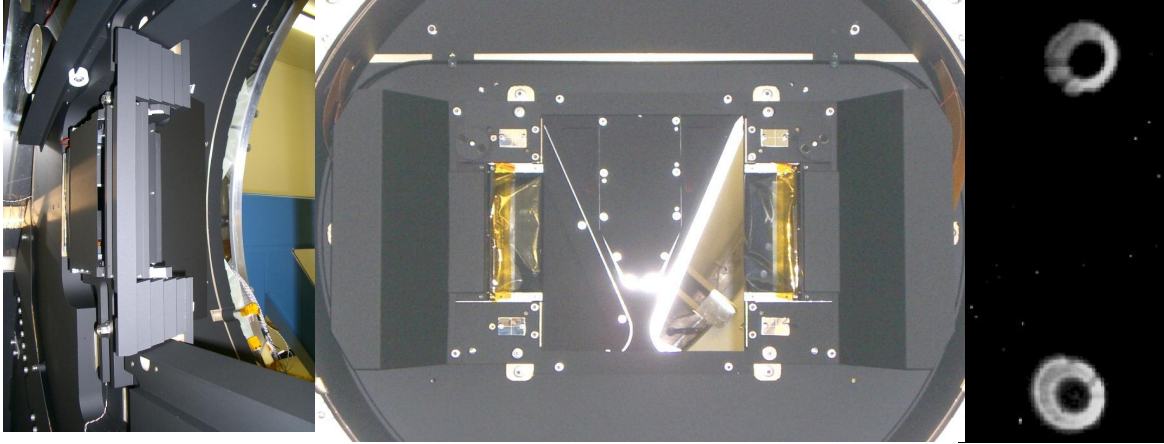


Figure 8: a) LOCS/AG unit seen from the rear, illustrating stray-light features. b) front view showing the locations of the pick-off mirrors relative to the science beam aperture in the WFS support plate. The filter wheel is positioned at one of the (blanked off) locations for the HOCS beam-splitter. c) Image of the test-source beam through the HOCS beam-splitter during testing, showing pre- and post-focal images.

7. IMAGING PERFORMANCE TESTS

In order to test the optical performance of the camera, a test beam was generated using two spherical mirrors as to generate an $f/3$ beam similar to the telescope, but augmented for different test configurations by pairs of cylindrical lenses to generate the correct aberrations that are present in the VISTA telescope optics and corrected by the camera optics. The same source is used without the cylindrical lenses to generate focused spots on the detectors when the lens barrel is not present in the cryostat. The source can be translated in focus and across the camera field of view, and so through-focus measurements of this point source are used to determine the co-planarity of the IR detectors and the LOCS/AG sensor CCDs.

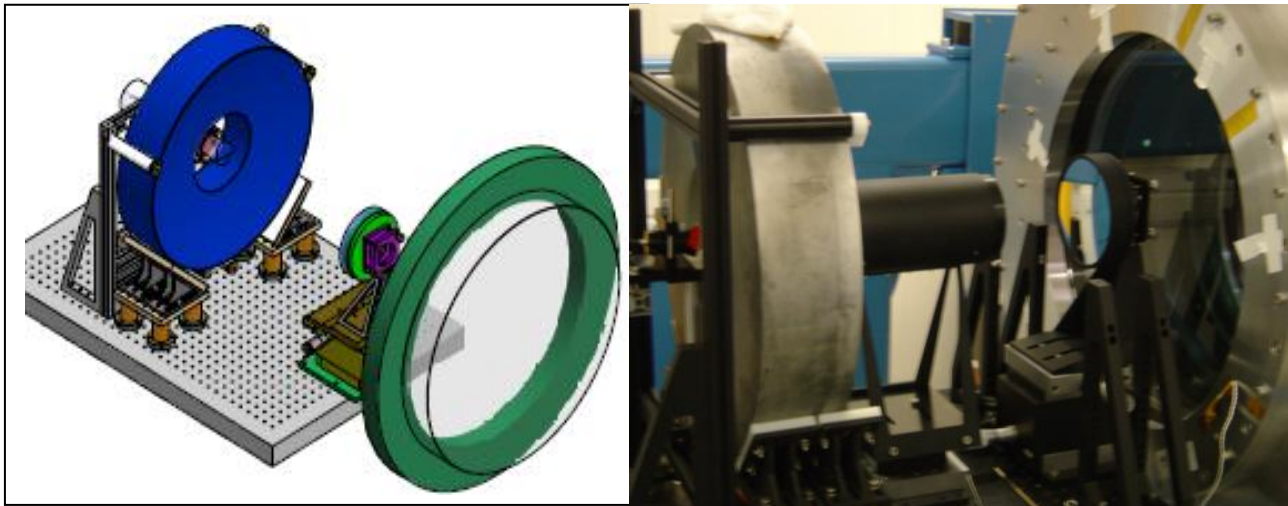


Figure 9: The test source used to evaluation of the camera imaging performance: a) basic configuration for focal plane co-planarity measurements. b) With cylindrical lenses included to generate the correct telescope aberrations for testing the camera image quality.

In practice, it proved difficult to locate a single pinhole exactly on the axis of the test source, and so instead we used a grid of 20 micron pinholes with 250 micron pitch. The effective field of view of the test source is about 1mm, and so this

arrangement guarantees that several holes in the grid will be well-corrected. Figure 10 shows typical images obtained by the IR detectors using this configuration.

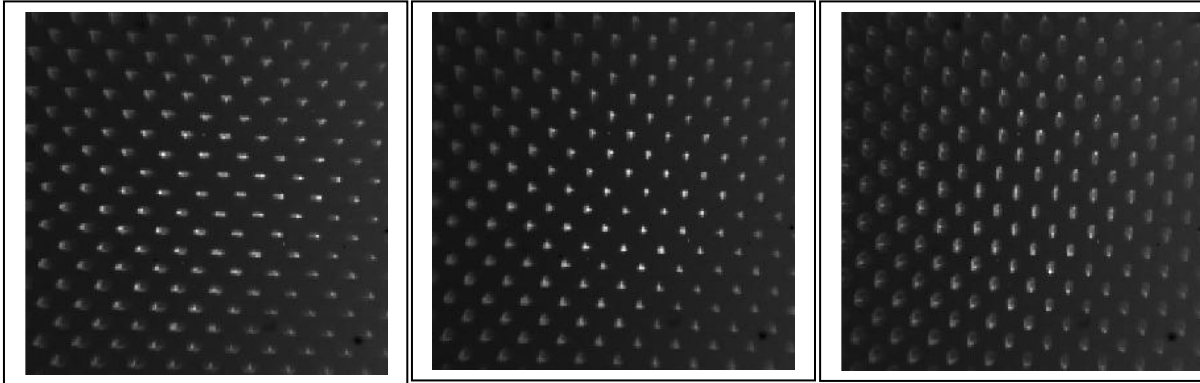


Figure 10: Example through focus images obtained from the test-source in the on-axis configuration (0.2mm steps in focus position).

8. SOFTWARE & TIMING PERFORMANCE

As noted previously, the large IR field of view provided by VISTA presents a challenge for the data acquisition software and hardware, in that the system is required to process and store one 256Mb data frame every 10s for up to 14 hours of observation. The IRACE system manages the 16 detectors as four separate arrays of four detectors each. The IRACE software delivers the data from the four arrays to a pair of dual CPU Linux-based PCs. Each PC handles the double correlated sampling and co-adding of the data from the arrays, in parallel threads. Each processing thread then transfers its data over Gigabit Ethernet to a third Linux-based PC, the instrument workstation, where information from the TCS and instrument monitoring software is added to the FITS header.

Recent timing tests using this setup with the VISTA TCS simulator for a series of 4000 5s exposures gave an average time per exposure of 10.66 seconds, of which there is 1 second reset, 1 second readout, and 5 seconds exposure, leaving 3.66 seconds for the data processing and transfer to the workstation disk, showing that the camera data handling infrastructure does indeed meet its expected capability of being able to start a new exposure within 5 seconds of the previous exposure being read out.

9. SCHEDULE AND PROSPECTS

The IR Camera is currently undergoing final assembly for all-up testing and provisional acceptance at the Rutherford Appleton Laboratory. Shipping to Paranal is expected to take place at the end of July 2006 on a schedule driven by the availability of the instrument preparation laboratory within the VISTA telescope enclosure (see McPherson et al. this conference). Engineering first light on VISTA is expected at the end of 2006 with handover of the full system to the Paranal observatory in spring of 2007.

10. ACKNOWLEDGEMENTS

VISTA is funded by grants from the UK Particle Physics and Astronomy Research Council and the UK Joint Infrastructure Fund, supported by the Office of Science and Technology and the Higher Education Funding Council for England, to Queen Mary University of London on behalf of the 18 University members of the VISTA Consortium of: Queen Mary University of London; Queen's University of Belfast; University of Birmingham; University of Cambridge; Cardiff University; University of Central Lancashire; University of Durham; University of Edinburgh; University of Hertfordshire; Keele University; Leicester University; Liverpool John Moores University; University of Nottingham;

University of Oxford; University of St Andrews; University of Southampton; University of Sussex; and University College London. We gratefully acknowledge assistance from Peter Biereichel, Joerg Stegmeier and Ezter Pozna at ESO for their help with our software timing tests.

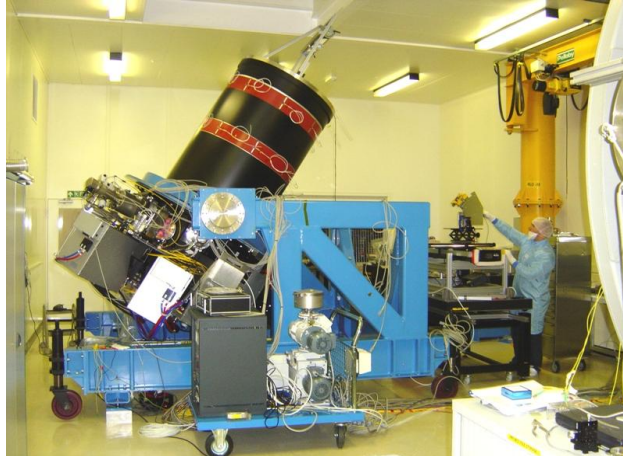


Figure 11: The Camera on its handling frame during flexure testing in the RAL AIV facility.

REFERENCES

1. J. P. Emerson *et al.*, "The Visible and Infra Red Survey Telescope for Astronomy: Overview". Proc SPIE **4836**, p.35-42 (2002).
2. A. McPherson *et al.*, "The VISTA project: a review of its progress and lessons learned developing the current programme", Proc SPIE **5489**, p.638 (2004).
3. E Atad-Ettinger *et al.*, "Optical design concept of the 4m Visible and Infra Red Survey Telescope for Astronomy". Proc SPIE **4842**, p.95-105. (2002).
4. P. J. Love *et al.*, "2k x 2k HgCdTe detector arrays for VISTA and other applications", Proc SPIE **5499**, p.68 (2004).
5. G. B. Dalton *et al.*, "The VISTA Infrared Camera". Proc SPIE **5492**, p.988-997 (2004).
6. P. Clark *et al.*, "Wavefront sensing within the VISTA infrared camera", Proc SPIE **5499** p.379 (2004).
7. D.L. Terrett, *et al.*, "Active optics and autoguiding control for VISTA", Proc SPIE **5496** p.129 (2004).
8. M. Caldwell *et al.*, "Aspects of concurrent design during the VISTA IR camera detailed design phase". Proc SPIE **5497**, p.51 (2004).
9. M. Meyer *et al.*, "ESO infrared detector high-speed array control and processing electronic IRACE". Proc SPIE **3354**, p.134 (1998).
10. P.J. Love *et al.*, "2K x 2K NIR HgCdTe Detector Arrays for VISTA and Other Applications.", AASL, **336**, 411 (2005).
11. N. Bezawada *et al.*, "Performance Overview of the VISTA IR Detectors", AASL, **336**, 499 (2005).
12. L. Mehrgan *et al.*, "256 Channel Data Acquisition System for VISTA Focal Plane to Readout Sixteen 2K x 2K Raytheon VIRGO Detectors", AASL, **336**, 601 (2005).